Available online at www.sciencedirect.com

ScienceDirect

Procedia Engineering 199 (2017) 3133–3138

Procedia Engineering

www.elsevier.com/locate/procedia

X International Conference on Structural Dynamics, EURODYN 2017

Interference of Vortex-Induced Vibration and Galloping: Experiments and Mathematical Modelling

Claudio Mannini[a,b,*], Tommaso Massai[a,b], Antonino Maria Marra[a,b], Gianni Bartoli[a,b]

[a] *Department of Civil and Environmental Engineering, University of Florence, Via S. Marta 3, 50139 Florence, Italy*
[b] *Inter-university Research Center on Building Aerodynamics and Wind Engineering (CRIACIV), Via S. Marta 3, 50139 Florence, Italy*

Abstract

This paper deals with the phenomenon of interference between vortex-induced vibration and transverse galloping, which occurs in the case of low-damped rectangular cylinders with a side ratio comprised between about 0.75 and 3. The results of a wide experimental campaign carried out in the wind tunnel are discussed, focusing on the key role played by the mass-damping parameter (Scruton number) of the oscillating body. It was found that a high value of the Scruton number is required to decouple completely the ranges of excitation due to vortex-induced vibration and galloping, and for the quasi-steady theory to predict correctly the galloping critical wind speed. Moreover, the problem is analytically addressed through a nonlinear wake-oscillator model, which is able to reproduce several features of the complicated phenomenon, provided that a crucial parameter is correctly calibrated.

Peer-review under responsibility of the organizing committee of EURODYN 2017.

Keywords: Galloping; Vortex-induced vibration; Vortex shedding; Rectangular cylinder; Wind tunnel tests; Mathematical modelling

1. Introduction

Bluff bodies with sufficient afterbody are prone to both vortex-induced vibration (VIV) and transverse galloping. For low enough values of the mass-damping parameter (Scruton number) of the oscillating system, the two phenomena can interfere, giving rise to an instability with peculiar features [1–3]. The interference phenomenon is not only physically interesting but also very important from the practical engineering point of view, as it may imply large-amplitude oscillations in flow speed ranges where no excitation is predicted by the classical theories for VIV and galloping [4]. Rectangular cylinders with a side ratio (streamwise-to-crossflow section lengths) approximately in the range 0.75 to 3 are susceptible to this combined excitation mechanism [2,5].

This paper discusses the data of a wind tunnel test campaign on the sectional model of a rectangular cylinder with a side ratio of 1.5, which is the cross section of two existing long-span steel arch structures [4], and which was found to be very prone to this phenomenon. Moreover, a nonlinear wake-oscillator model available in the literature was slightly modified and applied to the present test case. Promising results were obtained, and the differences were highlighted compared to the approach followed in the original work in which the model was presented.

* Corresponding author. Tel.: +39-055-275-8879 ; fax: +39-055-275-8800.
E-mail address: claudio.mannini@unifi.it

1877-7058
Peer-review under responsibility of the organizing committee of EURODYN 2017.
10.1016/j.proeng.2017.09.566

Nomenclature

A_1 slope in the origin of the quasi-steady transverse force coefficient
B streamwise section dimension of the prism (m)
C_D drag force coefficient ($C_D = 2F_D/\rho V^2 D$)
C_{Fy}^{QS} quasi-steady transverse force coefficient
C_L lift force coefficient ($C_L = 2F_L/\rho V^2 D$)
C_{L0} amplitude of oscillation of the lift coefficient due to vortex shedding
D cross-flow section dimension of the prism (m)
f lift coefficient per unit rotation of the equivalent wake lamina
F_D drag force per unit length (Nm^{-1})
F_L lift force per unit length (Nm^{-1})
h depth of the equivalent wake lamina (m)
h^* nondimensional depth of the equivalent wake lamina
l half length of the equivalent wake lamina (m)
l^* nondimensional half length of the equivalent wake lamina
L spanwise length of the prism (m)
M mass of the oscillating body (kg)
m^* fluid-to-solid mass ratio ($m^* = \rho D^2 L/2M$)
n_s vortex-shedding frequency (Hz)
n_0 still-air natural frequency of transverse vibration (Hz)
Re Reynolds number ($Re = \rho VD/\mu$)
Sc Scruton number ($Sc = 4\pi M\zeta_0/\rho BDL$)
St Strouhal number ($St = n_s D/V$)
U reduced flow speed ($U = V/n_0 D$)
U_g quasi-steady transverse galloping reduced flow speed ($U_g = 2BSc/A_1 D$)
U_r vortex-resonance reduced flow speed ($U_r = 1/St$)
V incoming flow speed (m/s)
V_{rel} relative incoming flow speed (m/s)
y transverse displacement of the oscillating prism (m)
Y nondimensional transverse displacement of the oscillating prism ($Y = y/D$)
α (relative) angle of attack of the incoming flow ($tan(\alpha) = -2\pi Y'/U$; rad)
μ air dynamic viscosity ($\mathrm{kgm}^{-1}\mathrm{s}^{-1}$)
ϑ inclination of the equivalent wake lamina (rad)
ρ air density ($\mathrm{kg/m}^3$)
υ ratio of U to U_r (or n_s to n_0)
ζ_0 mechanical critical damping ratio of the system
$(\cdot)'$ derivative with respect to nondimensional time $\tau = 2\pi n_0 t$
$(\cdot)_{rms}$ root-mean-square value of a variable

2. Wind tunnel study

2.1. Set-up

The phenomenon of interference has been extensively studied in the CRIACIV wind tunnel (Prato, Italy) with both static and aeroelastic tests. This open-circuit facility presents a rectangular test section 2.42 m wide and 1.60 m high, and the flow speed can be varied continuously up to 30 m/s. In the absence of turbulence generating devices, the

Fig. 1. View of the wind tunnel setup for the aeroelastic tests.

free-stream turbulence intensity is below 0.7%. Nevertheless, a few tests with grid-induced homogeneous isotropic turbulence were also performed.

A plywood sectional model, 986 mm long (L), 116 mm wide (B) and 77 mm deep (D), was used for both static and dynamic tests. To enforce bidimensional flow conditions, doubly symmetric rectangular plywood plates (450 mm × 150 mm × 4 mm) were provided at the model ends. The model was placed horizontally in the wind tunnel with the short side of the section perpendicular to the flow. The blockage ratio, calculated here as the ratio of the cross-wind section dimension of the model to the height of the wind tunnel, was 4.8%.

The measurements of the aerodynamic force coefficients at various angles of attack and of the Strouhal number were performed by means of two high-frequency six-component strain-gauges force balances placed at the ends of the model. The flow angle of attack was manually adjusted by means of an inclinometer with an accuracy of 0.05 deg.

In the aeroelastic set-up, the model was connected through its longitudinal axis-tube to two shear-type steel frames, the horizontal elements of which worked as plate-springs. Only the transverse (vertical) displacement was allowed by the two frames due to the very large in-plane bending stiffness of the vertical elements at which the model was connected. The suspension system was sheltered from wind by means of screens with streamlined noses, as shown in Fig. 1. The displacements of the model were recorded with two non-contact laser transducers. Without any additional dissipation device the critical damping ratio of the system was very low, well below 0.1%. It was also verified that the behavior of the plate springs was linear elastic up to the high oscillation amplitudes experienced by the model during the tests. The effective mass of the oscillating system resulted to be $M = 5.5$ kg, its stiffness 17.7 kN/m, and its natural frequency about 9 Hz.

The damping of the system was progressively increased through a device based on the electromagnetic induction principle, consisting of two aluminum plates, installed at the lateral sides of the oscillating system, moving between a pair of Neodymium magnetic disks. The development of eddy currents in the aluminum plates generated the desired damping force. The amount of external damping introduced into the system was varied by changing the distance between the magnets. Their linear behavior was checked through free-decay records after the release of large initial conditions. The additional dissipation forces allowed varying the Scruton number in small steps from low to large values, so to describe in detail the aeroelastic behavior of the system.

2.2. Results

The results of the static tests are reported in Fig. 2(a) in terms of the transverse force coefficient, calculated according to Fig. 3(a):

$$C_{Fy}^{QS}(\alpha) = sec(\alpha)[C_L(\alpha) + C_D(\alpha)\, tan(\alpha)] \tag{1}$$

It is well known that this coefficient is crucial to determine the aeroelastic behavior of a structure according to the quasi-steady theory [6], and in particular its slope in the origin is inversely proportional to the galloping critical flow speed U_g. In the present case, the high value of $A_1 = -dC_{Fy}^{QS}/d\alpha|_{\alpha=0}$ indicates a high proneness of the considered geometry to the galloping excitation.

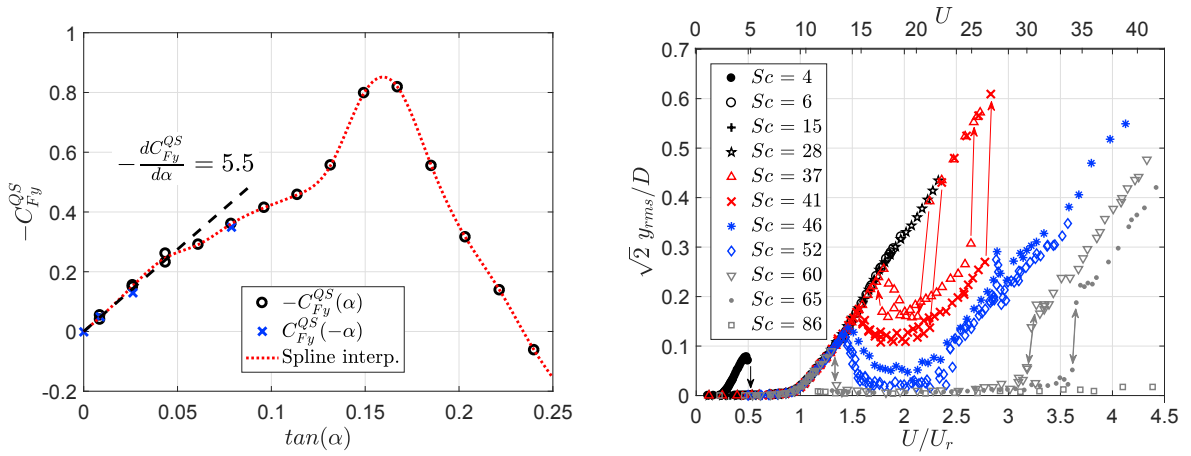

Fig. 2. (a) Transverse force coefficient determined through static tests and cubic spline interpolation (Re = 146,800); (b) amplitude-velocity curves measured in the wind tunnel for various Scruton numbers.

The results of the aeroelastic tests are summarized in Fig. 2(b), where the steady-state vibration amplitudes of the model as a function of the reduced flow speed are reported for various Scruton number values. It is clear that the main excitation of the model starts in the vortex resonance region ($U/U_r \cong 1$), and the oscillation amplitude increases with the flow speed in a nearly linear way. This trend is also kept for high amplitudes of vibration up to a Scruton number of at least 28, corresponding to an estimated value of U_g/U_r of about 1.6. By contrast, for $Sc = 37$ and 41 ($U_g/U_r = 2.2$ and 2.4), one can observe a decrease of the amplitude of oscillation for reduced velocities between about $1.5U_r$ and $2U_r$, followed by a recovery of the growth and then a large jump to a higher branch between $2.5U_r$ and $3U_r$. For even higher Scruton numbers ($Sc = 46$ and 52, corresponding to $U_g/U_r = 2.7$ and 3.0), around $U/U_r = 1.5$ one observes a decrease of the oscillation amplitude down to a low but non-null value, with quite irregular time histories. Then, the response progressively grows starting at a velocity slightly lower than $2.5U_r$. Finally, for the largest values of the mass-damping parameter considered here ($Sc = 60$, 65 and 86, corresponding to $U_g/U_r = 3.5$, 3.8 and 5.0), the vibration of the model sharply dies out slightly after the vortex-resonance flow speed, and a quasi-steady excitation appears with a jump at much higher wind velocities. In contrast, for low values of the Scruton number, when the galloping critical flow speed calculated with the quasi-steady theory is much lower than the vortex-resonance flow speed, no divergent instability occurs up to the vortex resonance flow speed. This implies a stabilizing effect of vortex shedding, despite the fact that from the quasi-steady standpoint the system should be unstable. This phenomenon, wherein the auto-periodic oscillation is suppressed by the hetero-periodic oscillation, is known as "asynchronous quenching" [7,8]. Only when the mechanical resonance triggers the oscillations, the cylinder starts to vibrate following an amplitude-velocity curve that however, unlike the classical VIV behavior, is not self-limited. Finally, the excitation observed at very low reduced flow speed ($U \lesssim 5$) for low values of the mass-damping parameter has been interpreted in [5] as a VIV excitation due to a secondary mechanism of vortex shedding.

Experiments in [5] showed that a low-intensity free-stream turbulence is able to enhance the tendency of vortex shedding and galloping to interfere in the transitional Scruton number range ($Sc \sim 40$). Further wind tunnel tests are underway to establish clearly the influence of incoming turbulence on the phenomenon, accounting for the aerodynamic effects reviewed in [9]. The first results show a reduction both in the Strouhal number and in the intensity of the vortex shedding, but also a more pronounced tendency of the cross section to get unstable because of galloping according to the quasi-steady theory (increase of the slope in the origin of the transverse force coefficient).

3. Mathematical modelling

An attempt has also been carried out to use a simple mathematical model to predict the main features of the interference mechanism. In particular, the model proposed in 1987 by Tamura and Shimada [10] has been considered

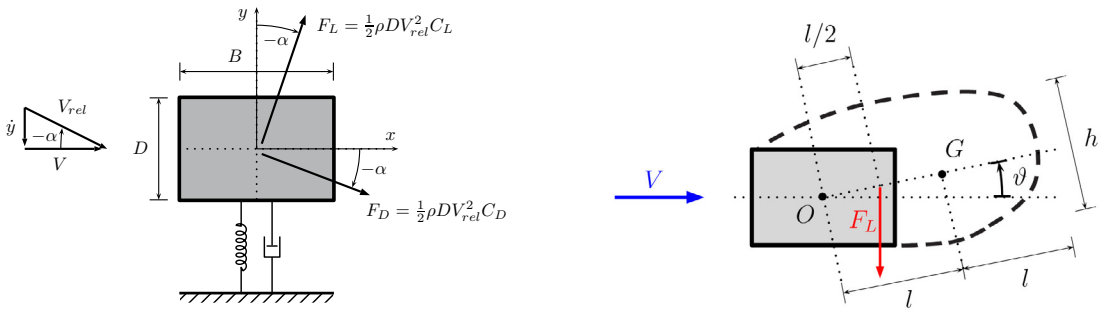

Fig. 3. (a) Determination of the transverse force for the vibrating rectangular cylinder with the quasi-steady approach; (b) schematic of the wake oscillator for the modified version of Tamura and Shimada's model.

herein. It is a two-equation wake-oscillator model relying on Birkhoff's concept about the oscillating wake [11], and on the viability of the linear superposition of unsteady-wake and quasi-steady forces acting on the oscillating body. The model formulation has been slightly modified here for theoretical reasons concerning the definition of the equivalent wake lamina (Fig. 3(b)), obtaining:

$$Y'' + 2\zeta_0 Y' + Y = -m^* \frac{U^2}{4\pi^2} f\left(\vartheta + \frac{2\pi Y'}{U}\right) - m^* \frac{U^2}{4\pi^2} C_{Fy}^{QS} \tag{2}$$

$$\vartheta'' - 2\beta\upsilon\vartheta'\left(1 - \frac{4f^2}{C_{L0}^2}\vartheta^2\right) + \upsilon^2\vartheta = -\lambda Y'' - \upsilon^2 \frac{2\pi Y'}{U} \tag{3}$$

$$\beta = \frac{f}{\sqrt{2}\pi^2 l^*} \tag{4}$$

$$\lambda = \frac{1}{l^*} \tag{5}$$

$$l^* = \frac{1}{8\pi S t^2 h^*} \tag{6}$$

Furthermore, the way to determine the parameter f has been changed, abandoning the analogy with the Magnus effect for a rotating circular cylinder followed in [10]. Conversely, f was estimated through a simple fit of the experimental data for a single response curve in the VIV range for a very high Scruton number value (in the case of no interference with the galloping excitation). The analysis emphasized the key role played by such a parameter, and revealed a previously unexplored behavior of the equations for high values of it. In particular, $f = 9$ was set in the equations, to be compared with $f = 1.16$ obtained through the analogy with the Magnus effect [10].

Results for intermediate values of the mass-damping parameter are reported in Fig. 4. The model is able to predict the dynamic response of the rectangular cylinder with satisfactory agreement with the experimental data. In particular, it captures the onset of the oscillations around the vortex-resonance flow speed and the nearly linear increase of the steady-state amplitude of the motion (Fig. 4(a)), without the large overshoot around the vortex resonance observed in [10], or in [12] with a similar mathematical model. In contrast, some limitations were observed in the Scruton number range for which transition in the interference phenomenon occurs, the numerical results overestimating the value of the mass-damping parameter up to which the amplitude-velocity curve monotonically increases (Fig. 4(b)).

4. Concluding remarks

The presented results clarify some features of the mechanism of interference between vortex shedding and galloping for a rectangular cylinder with a side ratio of 1.5. In particular, the quasi-steady theory fails to predict the threshold

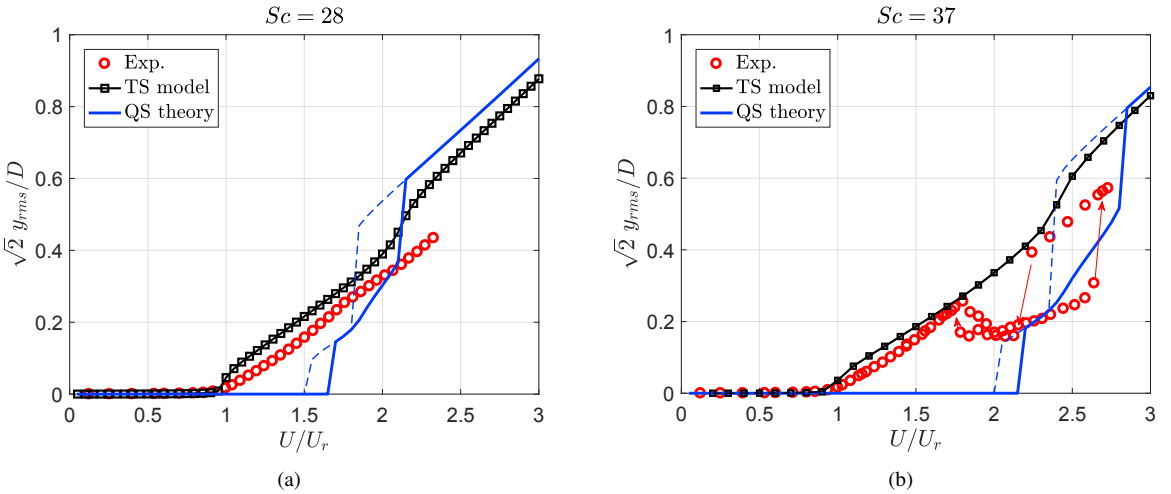

Fig. 4. Comparison between modified Tamura and Shimada's (TS) model, quasi-steady (QS) model and experiments for two Sc-number values.

velocity of galloping instability for values of the Scruton number lower than about 60 ($U_g/U_r \lesssim 3.5$). Moreover, high values of the Scruton number, say between 50 and 60 (normalized with the cross-section area), are needed to decouple completely the ranges of excitation due to vortex-induced vibration and galloping. This conclusion has an important impact on the engineering practice, since modern structures can easily be characterized by lower values of the Scruton number. Therefore, sustained vibrations can be encountered where they are not predicted by codes and standards, or by the classical theories of vortex-induced vibration and galloping.

In addition, the modeling of galloping occurring at low reduced flow speed and interfering with vortex shedding ("unsteady galloping") was attempted through a modified version of an existing model. This nonlinear wake-oscillator model, which also incorporates the quasi-steady force contribution, is able to reproduce the main features of the instability promoted by the interference of VIV and galloping, provided that a proper value of the coupling parameter f is set in the equations. This value is much higher than those ever tested in previous modeling efforts.

References

[1] G. V. Parkinson, M. A. Wawzonek, Some considerations of combined effects of galloping and vortex resonance, Journal of Wind Engineering and Industrial Aerodynamics 8 (1981) 135–143.
[2] C. Mannini, A. M. Marra, G. Bartoli, VIV-galloping instability of rectangular cylinders: Review and new experiments, Journal of Wind Engineering and Industrial Aerodynamics 132 (2014) 109–124.
[3] C. Mannini, A. M. Marra, G. Bartoli, Experimental investigation on VIV-galloping interaction of a rectangular 3:2 cylinder, Meccanica 50 (2015) 841–853.
[4] C. Mannini, M. Belloli, A. M. Marra, I. Bayati, S. Giappino, F. Robustelli, G. Bartoli, Aeroelastic stability of two long-span arch structures: A collaborative experience in two wind tunnel facilities, Engineering Structures 119 (2016) 252–263.
[5] C. Mannini, A. M. Marra, T. Massai, G. Bartoli, Interference of vortex-induced vibration and transverse galloping for a rectangular cylinder, Journal of Fluids and Structures 66 (2016) 403–423.
[6] G. V. Parkinson, N. P. H. Brooks, On the aeroelastic instability of bluff cylinders, Journal of Applied Mechanics 28 (1961) 252–258.
[7] N. Minorsky, Introduction to Non-Linear Mechanics: Topological Methods, Analytical Methods, Non-Linear Resonance, Relaxation Oscillations, J. W. Edwards, Ann Arbor, MI, 1947.
[8] T. V. Santosham, Force measurements on bluff cylinders and aeroelastic galloping of a rectangular cylinder, Master's thesis, University of British Columbia, Vancouver, Canada, 1966.
[9] C. Mannini, A. M. Marra, L. Pigolotti, G. Bartoli, The effects of free-stream turbulence and angle of attack on the aerodynamics of a cylinder with rectangular 5:1 cross section, Journal of Wind Engineering and Industrial Aerodynamics 161 (2017) 42–58.
[10] Y. Tamura, K. Shimada, A mathematical model for the transverse oscillations of square cylinders, in: Proceedings of the 1st International Conference on Flow Induced Vibrations, May 12-14, 1987, Bowness-on-Windermere, UK, Springer-Verlag, 1987, pp. 267–276.
[11] G. Birkhoff, Formation of vortex streets, Journal of Applied Physics 24 (1953) 98–103.
[12] R. M. Corless, G. V. Parkinson, A model of the combined effects of vortex-induced oscillation and galloping, Journal of Fluids and Structures 2 (1988) 203–220.